

Interfaces between Lead and Amorphous Matrices in Immiscible Alloy Systems

Alok Singh^{1*} and A.P. Tsai^{1,2},

¹*National Institute for Materials Science, 1-2-1 Sengen, Tsukuba 305-0047, Japan*

²*Institute for Multidisciplinary Research in Advanced Materials, Tohoku University, Sendai, Japan*

(Received June 29, 2010)

ABSTRACT

Interfaces between solid lead and amorphous matrix are described, with experimental data from system of lead particles embedded into Al-Cu-V amorphous matrix. Since the structure of the amorphous matrix cannot be described with surety, it has been approached by taking known factors in account, such as the relative stability of various facets of lead and its interfaces with quasicrystals. Lead particles take a round shape in accordance with the amorphous matrix, and are often twinned to form more uniform facets (with uniform energy) on the surface/interface. Interface stability of the lead particles is indicated by their melting and solidification behavior. Therefore melting and solidification behavior of the embedded particles in amorphous matrix has been compared with those in crystalline and quasicrystalline matrices.

1. INTRODUCTION

Interfaces are crucial in determining the properties of materials, whether they are mechanical properties or physical. The effect of interfaces becomes more prominent when the size scale becomes smaller, down to nanometric. A good indicator of the stability of interfaces is given by the melting and solidification

behavior of the materials. To study these, nano-particles are often embedded into a matrix by rapid solidification, taking advantage of phase immiscibility [1,2]. As the particle size becomes smaller, the ratio of surface area to volume becomes larger. Consequently, the structure of the surface or interfaces of the particles play a larger role in their melting and solidification. This is especially so because melting begins at the surface/interface, and nucleation of solidification occur easily on surfaces. The melting temperature of free particles decreases when their size becomes very fine, to less than 20nm. In case of embedded particles, the melting temperature may show a superheating, if the particles make coherent interfaces with the matrix.

In case of particles embedded in a crystalline matrix, interface epitaxy suppresses the vibration motion of the interface atoms and therefore suppresses melting in accordance with the Lindemann criterion. In an amorphous matrix, epitaxy is not possible, which results in a different melting and solidification behavior.

The case of crystalline particles embedded in an amorphous matrix is very interesting. However, it is also more difficult as the structure of the interfaces cannot be determined directly. In this paper, the structure of the interfaces between lead particles and an amorphous matrix has been explored by various direct and indirect means. Experimental observations are from lead nano-particles embedded in an Al-Cu-V amorphous matrix.

* Correspondence: Alok.Singh@nims.go.jp

2. INTERFACES OF LEAD PARTICLES IN CRYSTALLINE MATRIX

Lead forms immiscible systems with a large number of elements of higher melting temperatures. Due to this, it can be embedded into these elements such as in aluminum /3,4/, copper /4,5/ and zinc /6/. By embedding particles in a matrix, the effect of their shape and size can be studied on melting and solidification. Goswami and Chattopadhyay have studied lead nano-particles embedded in four close-packed structures of aluminum, copper, nickel and zinc /4/. In copper and aluminum, the orientation relationship is cube-on-cube, $(111)_{\text{Pb}} \parallel (111)$ and $[1\bar{1}0]_{\text{Pb}} \parallel [1\bar{1}0]$. The shape of lead particles in these matrix is truncated cuboctahedron. In nickel it followed the orientation relationship $(100)_{\text{Pb}} \parallel (100)_{\text{Ni}}$ and $[011]_{\text{Pb}} \parallel [001]_{\text{Ni}}$, with a rough cuboctahedron morphology. Many of the particles embedded in Ni were not single crystals but had 2 or 3 domains.

In case of embedding in zinc, a $(111)_{\text{Pb}}$ plane is parallel to the hexagonal (0001) plane of zinc /6/. The morphology of the embedded lead particles was truncated hexagonal biprism. Significantly, changes in the morphology could occur on annealing treatments, which could change the melting behavior of the particles. It is reported in case of Pb-Zn that growth of some facets occurs and the interfaces became very sharp when an annealing treatment is carried out at a temperature below the melting temperature of lead. This resulted in a superheating of 62K in some lead particles /6/.

To understand the effect of various faceting, it is important to understand the behavior of each facet. Grabaek et al. /7,8/ showed that the superheating of lead particles embedded in aluminum is due to the facets on $\{111\}$ and $\{100\}$ planes. Pluis et al. /9/ determined that $\{111\}$ and $\{100\}$ planes of a free Pb crystal melt the last, showing a superheating, while melting of $\{110\}$ planes starts 40K below the bulk melting temperature. In case of embedded particles, epitaxial interfaces are expected to show superheating. Favorable orientations of the embedded crystal in a matrix match close packed planes of the two phases at the interfaces.

When the interface is not planar but irregular, its stability is low and leads to a lower melting temperature

of the particles /10,11/. Such interfaces form by such processing as mechanical milling of powders.

3. INTERFACES OF LEAD PARTICLES IN QUASICRYSTALLINE MATRIX

The lead particles could be embedded into Al-Cu-Fe stable icosahedral quasicrystalline phase because lead forms immiscible system with aluminum, copper as well as iron. The lead particles embedded in the quasicrystalline matrix did not look sharp but rounded. This was due to the high symmetry of the icosahedral phase. It was found that the facets of the matrix icosahedral phase were on its five and twofold planes, which are known to be the closest packed planes /12,13/. An icosahedral phase has a set of six fivefold and fifteen twofold planes. The lead particle facets were mostly on its $\{111\}$ and $\{110\}$ planes. More than one orientation relationship were found, which tended to match these close packed planes of lead with the high symmetry planes of the matrix. Major orientation relationships are (1) $\langle 111 \rangle_{\text{Pb}} \parallel 2f$, $\{110\}_{\text{Pb}} \parallel 5f$, (2) $\langle 111 \rangle_{\text{Pb}} \parallel 2f$, $\{100\}_{\text{Pb}} \parallel 5f$; (3) $\langle 100 \rangle_{\text{Pb}} \parallel 2f$, $\{012\}_{\text{Pb}} \parallel 5f$ and (4) $\langle 110 \rangle_{\text{Pb}} \parallel 2f$, $\{111\}_{\text{Pb}} \parallel 5f$. There are many possibilities of planar matches due to the high symmetry of the icosahedral phase. Moreover, due to quasiperiodicity, there is a high likelihood of matching of interplanar spacings too. A detailed description of crystal-quasicrystal interfaces is given elsewhere /14/. In case of crystalline particles embedded into a crystalline matrix, the particles take definite shapes usually dictated by the intersection symmetry of the two phases. Due to these well defined shapes, the crystallographic orientation of the particles can judged easily. However, in case of crystalline particles embedded in a quasicrystalline matrix, even though facets occur on definite planes, the particles do not have uniform shapes. This is because faceting may not be on all fivefold and twofold planes. There being many fivefold and twofold planes, the shape appears rounded. All facets can be recognized only by tilting of the samples. Due to a much higher symmetry of the matrix quasicrystal phase, embedded particles with the same orientation relationship with the matrix can take various

orientations. This is compounded by the fact that more than one orientation relationships occur. This situation is in between that of crystalline particles embedded in a crystalline matrix and that of an amorphous matrix.

4. INTERFACES OF LEAD PARTICLES IN AMORPHOUS MATRIX

Metallic amorphous matrices can be made of alloys containing two or more elements. Dispersion of nano-particles of elements such as bismuth and lead can be made by virtue of the fact that bismuth and lead are immiscible in many elements in the liquid state.

An example of embedding of bismuth particles in an amorphous matrix was shown by Goswami and Chattopadhyay /15/ by controlling the nucleation of the phase separating liquid prior to solidification. Bismuth has liquid immiscibility in binary states with elements aluminum, iron and silicon. Addition of iron to Al-Si stabilizes the melt and promotes formation of metallic glass by rapid solidification. A known glass forming composition is $\text{Al}_{65}\text{Si}_{15}\text{Fe}_{20}$. Melting this alloy with about 7at%Bi, and rapid solidification by melt-spinning produced crystalline rhombohedral bismuth particles of size 5 to 30 nm in a glassy matrix. In the as-solidified condition, the bismuth particles were single crystals. However, after a thermal cycling above the melting temperature of bismuth, the particles showed multiple crystallographic domains. It has been argued that the formation of multiple domains in the particles occurs to preserve the symmetry of the initial liquid cavity without the loss of continuity at the interface. Multiplication of domains resulted in lowering of the melting temperature of the bismuth particles due to size effect.

Similarly, lead particles have been embedded in Al-Cu-V amorphous matrix /16/. $\text{Al}_{75}\text{Cu}_{15}\text{V}_{10}$ is known to yield metallic glass on rapid solidification /17/. Lead is immiscible in all these three constituent elements in liquid as well as solid form.

The $\text{Al}_{75}\text{Cu}_{15}\text{V}_{10}$ metallic glass is known to transform to a quasicrystalline (QC) state on annealing /17/. In our studies, it was found that this transformation occurs at 718.8K on heating at a constant rate in a DSC

/16/. Eventually, the alloys transforms to a crystalline state on prolonged heating close to melting temperature, where it transforms to Al_2Cu and Al_3V phases /17/. An intermediate icosahedral QC state indicates that the amorphous state may also have icosahedral short range order.

In as fabricated condition by rapid solidification, lead particles of size about 30nm were uniformly distributed in an amorphous matrix of $\text{Al}_{75}\text{Cu}_{15}\text{V}_{10}$, as shown in **Figure 1a**. The lead particles had round shape and were often twinned on {111} planes, **Figure 2**.

On solidification of the alloy system, the matrix solidifies first. Liquid drops of lead are trapped in this solidified matrix. Since liquid (lead in this case) has no shape, the facet formation occurs according to the crystallographic symmetry of the matrix phase. In case of amorphous matrix, there is no faceting but a round shape. When the liquid droplets of lead solidify, there is no apparent lattice match across the interface. In such a case, a lowering of interface energy can occur by formation of interface with low energy /close-packed planes of the lattice. In order to maximize the surface area with low energy planes, twinning can occur. It is observed in Fig. 2 that by twinning, the total symmetry of the particle is increased and the interface is on similar lattice planes all over.

5. EFFECT OF Al-Cu-V AMORPHOUS AND QUASICRYSTALLINE MATRIX ON THE MELTING AND SOLIDIFICATION OF LEAD NANOPARTICLES

Heating experiments in DSC (**Figure 3**) indicated that these lead particles were stable upto 573K, after which they started melting. Beginning at 573K, a melting shallow endothermic peak was observed at about 583K. Another peak which was very sharp occurred at the bulk melting temperature of lead, 600K. In order to create stable interfaces between solid lead and the amorphous matrix, long term annealings were performed at 553K. After annealing at even 400h, the shape of the particles remained the same and existence of twinning persisted, **Figure 1b**.

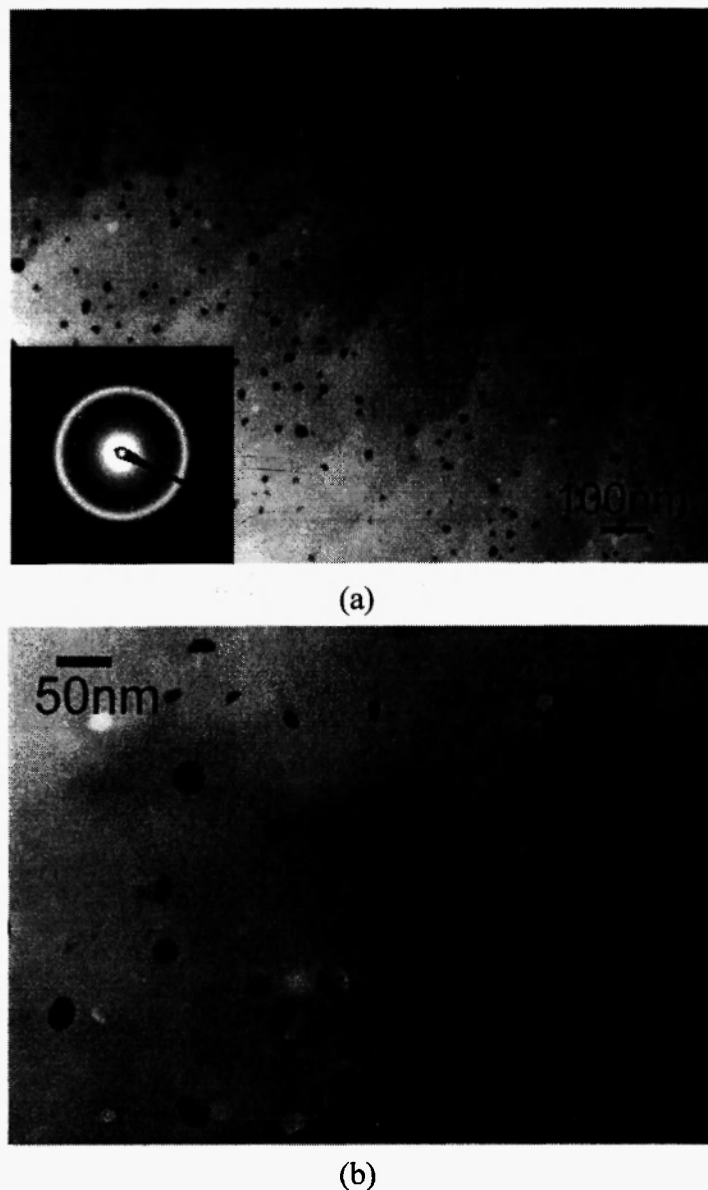


Fig. 1: TEM bright field micrographs showing lead particles embedded in Al-Cu-V matrix after (a) melt-spinning and (b) followed by annealing at 553K

Upon cooling after melting, no clear exothermic peak indicating solidification was observed [16]. This indicates that solidification of the lead nanoparticles occurs over a large temperature range. No clear peak can also be seen as a very broad peak, which indicates a large contact angle of solid nucleus on the matrix interface [18,19]. A large contact angle is associated with high interfacial energy.

Repeated heating and cooling runs in DSC were

performed to determine the number of particles solidified by their melting peaks [16]. It showed that more than half of the particles which melt at the bulk melting temperature of lead solidify by cooling to 563K, and all of them solidify by 523K [16]. The particles which melt below the bulk melting temperature start solidify below 563K and continue to solidify below 523K. Thus an undercooling of over 100K occurs.

On heating to higher temperatures, the matrix first

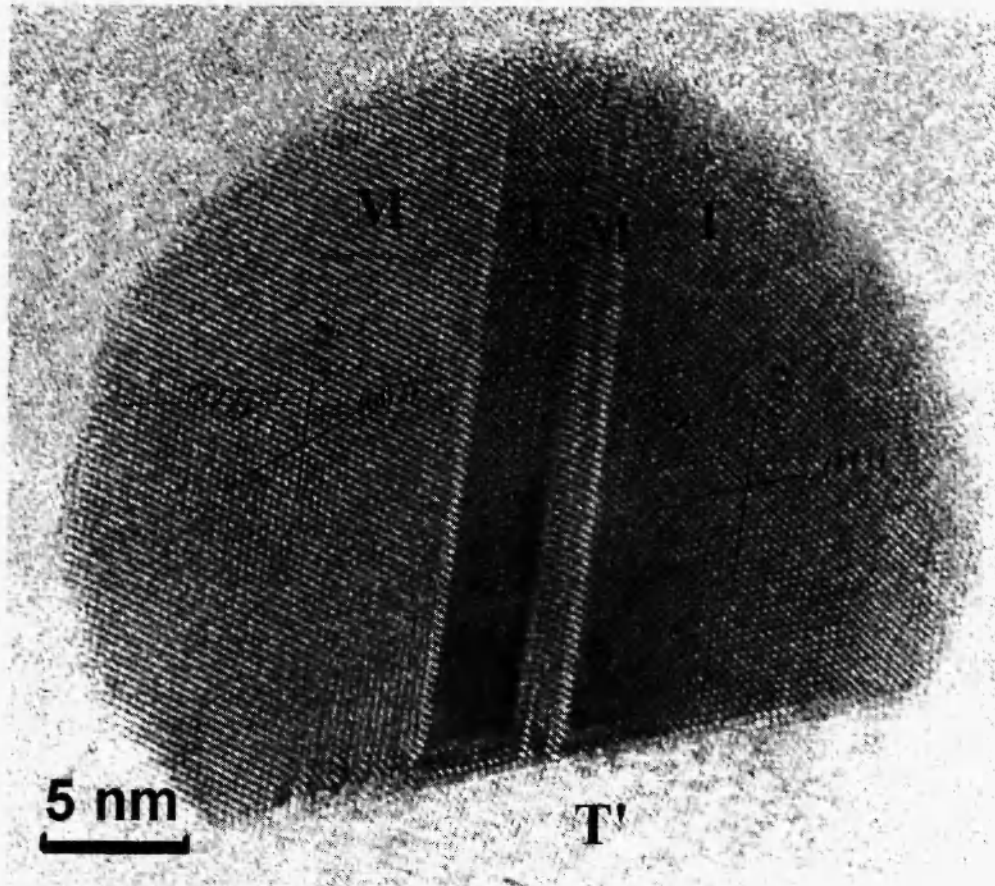


Fig. 2: A lead particle embedded in the amorphous matrix showing twins /16/

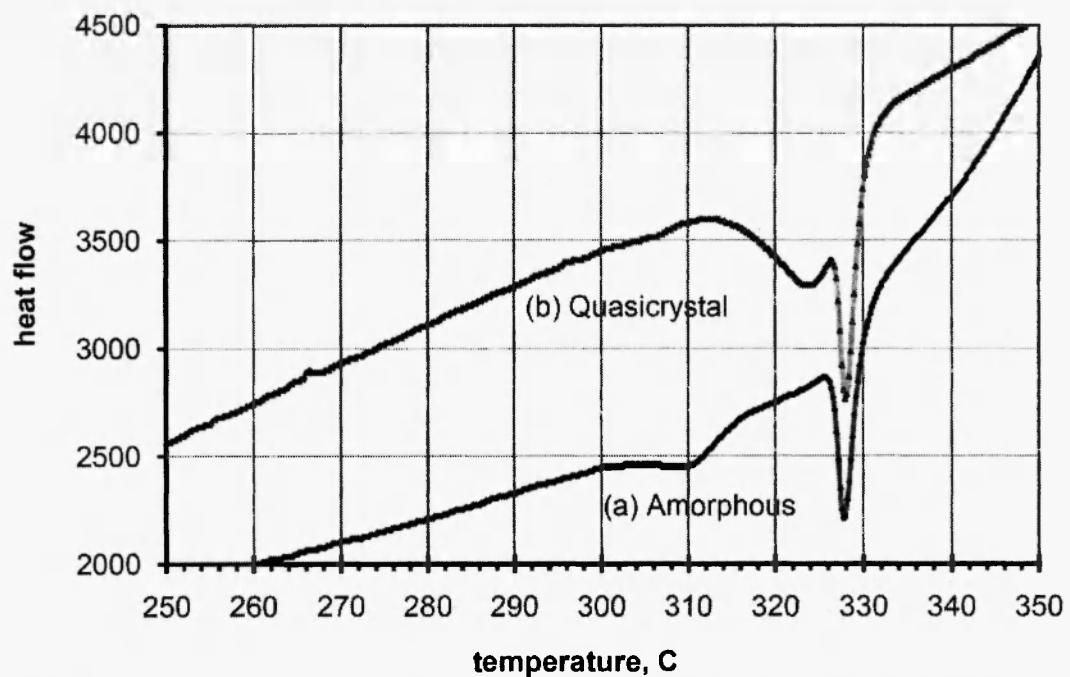


Fig. 3: Part of DSC curves showing melting endotherms of the melting of lead particles embedded in (a) amorphous Al-Cu-V matrix and (b) after the matrix is transformed to quasicrystalline state

transforms to a metastable icosahedral quasicrystalline phase before transforming to crystalline phases. This indicates that the structure of this icosahedral phase is closer to the amorphous phase. In other words, the amorphous phase must have strong icosahedral order. It is therefore instructive to observe the melting and solidification of the same lead particles in this matrix. After measuring the melting and solidification temperatures of lead particles in the amorphous matrix in DSC (**Figure 3a**), the sample was heated to 773K, by which the matrix transformed to the icosahedral state [16]. The microstructure after this treatment showed that the lead particles were still twinned (**Figure 4**). In subsequent cooling and heating run, two melting peaks were obtained – one at the bulk melting temperature of lead, and another at a lower temperature with onset at

about 585K and peak at 597K (**Figure 3b**). Thus the onset of melting becomes 12K higher, and peak of the lower peak about 14K higher.

Repeated melting and solidification runs in DSC showed that nearly all of the lead particles with lowered melting temperature start solidifying below 523K (i.e., undercooling of larger than 77K). About half of those particles which melt at the bulk melting temperature solidify by 563K, and all by 523K, similar to the case of the amorphous matrix. Thus the melting and solidification behavior of the particles which melted at the bulk melting temperature of lead remained the same in each matrix. The behavior of the particles which showed lowered melting temperatures changed from the amorphous matrix to the icosahedral matrix. The melting temperature was raised by about 12K.

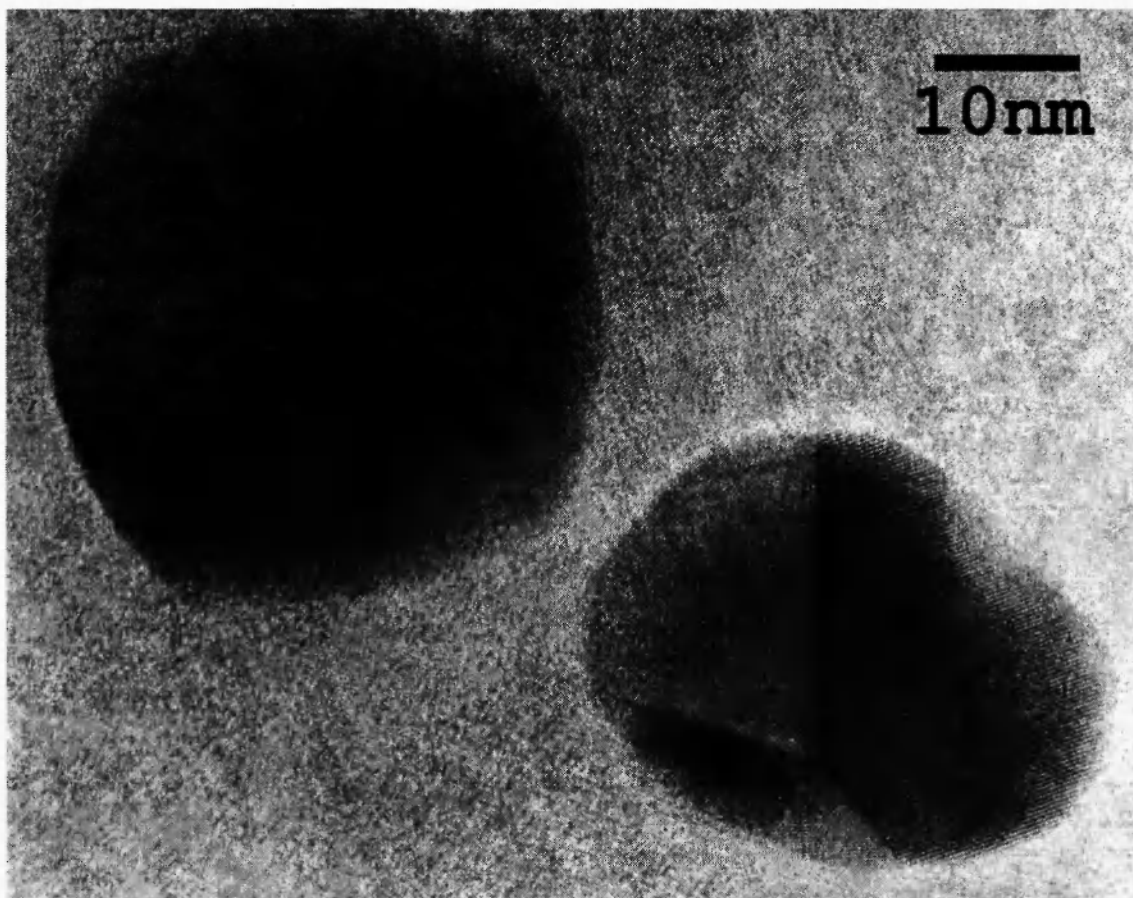


Fig. 4: Lead particles in Al-Cu-V quasicrystalline matrix

6. INTERFACIAL ENERGIES

Relative interfacial energies can be estimated from the melting and solidification behavior. Thermodynamically, for free particles a change in the melting temperature is given by /20,21/

$$\Delta T \propto \frac{T_m}{L_f} \left[\gamma_{LV} \left(\frac{\rho_s}{\rho_L} \right)^{2/3} - \gamma_{SV} \right] \quad (1)$$

Where T_m is the bulk melting temperature, L is the latent heat of fusion (per unit volume), ρ_s and ρ_L are densities of solid and liquid phases, and γ_{LV} and γ_{SV} are interfacial energies of liquid-vapor and solid-vapor interfaces. The relative energies of γ_{LV} (solid-liquid), γ_{LV} and γ_{SV} interfaces determine superheating or supercooling. If $\gamma_{SV} < \gamma_{LV} + \gamma_{LV}$, superheating is possible.

In case of embedded particles, the vapor phase is replaced by the matrix phase, and the relevant interfacial energies are γ_{SL} , γ_{LM} and γ_{SM} , where M denotes the matrix. An expression similar to (1) is given as /22/

$$\Delta T \propto \frac{3T_m}{L_f} [\gamma_{LM} - \gamma_{SM}] \quad (2)$$

Structurally a crystalline phase is very different from amorphous, and therefore their interface energy γ_{SM} will be high. On the other hand, a liquid is believed to be closer in structure to amorphous, and therefore their interface γ_{LM} will have lower value. Therefore, $\gamma_{LM} < \gamma_{SL} + \gamma_{SM}$, and a lowering of melting temperature, and an undercooling on solidification is expected. Icosahedral order maybe closer in structure to the amorphous and the liquid phase, but does form matching interfaces with crystalline phases, and therefore γ_{SM} is lower. The Al-Cu-V icosahedral phase is reported to have a high degree of defects, so that its structure is described by an icosahedral glass model /23,24/. The interfacial energy between amorphous and icosahedral phase in Al-Cu-V is estimated to be very low /25/.

There need not always be a lowering of melting temperature of crystalline nano-particles embedded in

an amorphous matrix. Germanium nanocrystals (5 nm size) embedded into silica substrate by ion implantation showed melting-solidification hysteresis centered on the bulk melting temperature of germanium /22/ (even though free germanium nanocrystals show typical lowering of melting temperature /26/. This is explained by the difference $\gamma_{LM} - \gamma_{SM}$. For $\gamma_{LM} - \gamma_{SM} = 0$, the contact angle is 90° and the hysteresis loop is symmetrical about the bulk melting temperature. The width of the hysteresis loop is determined by γ_{SL} .

This can also be discussed by considering example of a quasicrystal matrix. In case of crystal-crystal interfaces epitaxy can be obtained if the matching planes on either side of the interface have similar interplanar spacing. It has been shown that epitaxy is not a property of periodic planes alone, but can be extended to quasicrystal-crystal interfaces too /27/. This epitaxy can be observed as coincidence of reciprocal spots in diffractions. In fact, quasiperiodic planes can form epitaxy with a wide range of crystalline planes. Quasiperiodicity generates a number of interplanar spacings not multiples of each other. In Al-Cu-V it appears that the amorphous phase structure may have closeness to the quasiperiodic structure /25/, hence some kind of epitaxial nature can be expected.

7. CONCLUSIONS

Interfaces of crystalline particles embedded in an amorphous matrix are described by considering example of lead particles embedded into amorphous Al-Cu-V matrix prepared by rapid solidification. In this alloy system, transformation of the amorphous phase on annealing at high temperature first leads to formation of a metastable icosahedral quasicrystalline phase. The nature of this quasicrystalline phase has been reported to be similar to its parent amorphous phase. With respect to morphology and orientations, the nature of crystalline particles embedded in quasicrystalline matrix is in between those embedded in crystalline and amorphous matrices. Crystalline particles embedded in amorphous phase matrix take round shapes. They are often twinned to form interfaces with more uniform energy. The energy of the interfaces is explored by considering the

melting and solidification behavior of the embedded particles studied by DSC. A weak epitaxial nature is not ruled out.

REFERENCES:

1. G. C. Wang and C. S. Smith, *Trans. AIME*, **188**, 136 (1950).
2. R. T. Southin and G. A. Chadwick, *Acta Metall.*, **26**, 223 (1978).
3. K.I. Moore, W.T. Kim and B. Cantor, *Acta metal. mater.*, **38**, 1327 (1990).
4. R. Goswami and K. Chattopadhyay, *Acta metal. Mater.*, **43**, 2837 (1995).
5. W.T. Kim and B. Cantor, *Acta metal. Mater.*, **40**, 3339 (1992).
6. R. Goswami and K. Chattopadhyay, *Phil. Mag. Lett.*, **68**, 215 (1993).
7. L. Grabaek, J. Bohr, E. Johnson, A. Johansen, L. Sarholt-Kristensen and H.H. Andersen, *Phys. Rev. Lett.*, **64**, 934 (1990).
8. L. Grabaek, J. Bohr, H.H. Andersen, A. Johansen, E. Johnson, L. Sarholt-Kristensen and I.K. Robinson, *Phys. Rev. B*, **45**, 2628 (1992).
9. B. Pluis, A.W. Denier van der Gon, J.W.M. Frenken and J.F. van der Veen, *Phys. Rev. Lett.*, **59**, 2678 (1987).
10. H.W. Sheng, K. Lu and E. Ma, *Acta mater.*, **46**, 5195 (1998).
11. H. Rosner and G. Wilde, *Scripta Materialia*, **55**, 119 (2006).
12. A. Singh and A.P. Tsai, *Phil. Mag. Lett.*, **77**, 89 (1998).
13. A. Singh and A.P. Tsai, *Acta mater.*, **46**, 4641 (1998).
14. A. Singh and A.P. Tsai, *J. Phys.: Condens matter.*, **20**, 314002 (2008).
15. R. Goswami and K. Chattopadhyay, *Appl. Phys. Lett.*, **69**, 910 (1996).
16. A. Singh and A.P. Tsai, *Jpn. J. Appl. Phys.*, **39**, 4082 (2000).
17. A.P. Tsai, A. Inoue and T. Masumoto, *Jap. J. Appl. Phys.*, **26**, L1994 (1987).
18. W.T. Kim, D.L. Zhang and B. Cantor, *Metall. Trans.*, **A 22**, 2487 (1991).
19. R. Goswami & K. Chattopadhyay, *Acta Mater.*, **44**, 2421 (1996).
20. K. J. Hansen, *Z. Phys.*, **157**, 523 (1960).
21. P. R. Couchman and W. A. Jesser, *Nature (London)*, **269**, 481 (1977).
22. Q. Xu, I.D. Sharp, C.W. Yuan, D.O. Yi, C.Y. Liao, A.M. Glaeser, A.M. Minor, J.W. Beeman, M.C. Ridgway, P. Kluth, J.W. Ager III, D.C. Chrzan and E.E. Haller, *Phys. Rev. Lett.*, **97**, 155701 (2006).
23. A.P. Tsai, K. Hiraga, A. Inoue, T. Masumoto and H.S. Chen, *Phys. Rev. B*, **49**, 3569 (1994).
24. P.W. Stephen and A.I. Goldman, *Phys. Rev. Lett.*, **56**, 1168 (1986).
25. J.C. Holzer and K.F. Kelton, *Acta metal. Mater.*, **39**, 1833 (1991).
26. N.T. Gladkich, R. Neidermayer and K. Spiegel, *Phys. Status Solidi*, **15**, 181 (1966).
27. W. Theiss and K.J. Franke, *J. Phys.: Condens matter.*, **20**, 314004 (2008).